Journal of Analytical Sciences, Methods and Instrumentation, 2015, 5, 59-65
Published Online December 2015 in SciRes. http://www.scirp.org/journal/jasmi
http://dx.doi.org/10.4236/jasmi.2015.54007

Determination of N and O-Atoms, of $N_2(A)$ and $N_2(X, v > 13)$ Metastable Molecules and N_2^+ Ion Densities in the Afterglows of Ar-N_2 Microwave Discharges

Andre Ricard, Hayat Zerrouki, Jean-Philippe Sarrette

Laplace, Toulouse, France
Email: ricard@laplace.univ-tlse.fr

Received 5 November 2015; accepted 14 December 2015; published 17 December 2015

Abstract

Early afterglows of Ar-N_2 flowing microwave discharges are characterized by optical emission spectroscopy. The N and O atoms, the $N_2(A)$ and $N_2(X, v > 13)$ metastable molecules and N_2^+ ion densities are determined by optical emission spectroscopy after calibration by NO titration for N and O-atoms and measurements of NO and N_2 band intensities. For an Ar-xN_2 gas mixture with × increasing from 2 to 100% at 4 Torr, 100 Watt and an afterglow time of 3 × 10^{-3} s at the 5 liter reactor inlet, it is found densities in the ranges of (2 - 6) × 10^{14} cm^{-3} for N-atoms, one order of magnitude lower for $N_2(X, v > 13)$ and for O-atoms (coming from air impurity), of 10^{10} - 10^{11} cm^{-3} for $N_2(A)$ and of 10^8 - 10^9 cm^{-3} for N_2^+.

Keywords

Ar-N_2 Microwave Discharge, Flowing Afterglow, N-Atoms, N_2 Metastables, N_2^+ Ions

1. Introduction

Afterglows of N_2 flowing microwave discharges have been studied at medium gas pressures (1 - 20 Torr) for sterilization of medical instruments by N-atoms [1] [2]. The mentioned project of sterilization in N_2 afterglow is based on N-atom etching of bacteria without oxidation by O-atoms. A part of the present study is to detect the O-atoms from air impurity to appreciate their influence on the sterilization process.

The main part concerns a study of Ar-N_2 gas mixtures to enhance the sterilization process in the early after-

How to cite this paper: Ricard, A., Zerrouki, H. and Sarrette, J.-P. (2015) Determination of N and O-Atoms, of $N_2(A)$ and $N_2(X, v > 13)$ Metastable Molecules and N_2^+ Ion Densities in the Afterglows of Ar-N_2 Microwave Discharges. *Journal of Analytical Sciences, Methods and Instrumentation*, **5**, 59-65. http://dx.doi.org/10.4236/jasmi.2015.54007

glow. The interest of N_2 dilution into Ar is to increase the electron energy in the plasma at constant values of transmitted power and of gas pressure. Superelastic collisions of electrons on the Ar metastable atoms produced in the plasma could enhance the electron energy. It is mentioned here that in the present measurements of flowing afterglow, the Ar metastable atoms have disappeared after collisions on the tube wall (destruction probability of about 1). As a consequence, the excitation transfers of Ar metastable atoms on N_2 can be discarded at a distance of about 1 cm after the discharge end. Another interest of Argon dilution is to maintain the plasma at high gas pressure, up to the atmospheric gas pressure while keeping a plasma power as low than 100 Watt [3].

The early flowing afterglows produced from Ar-N_2 microwave plasmas are presently studied by emission spectroscopy with the same experimental methods as in N_2-H_2 RF afterglow [4] [5], in N_2, N_2-O_2 [6] and in N_2-H_2, Ar-N_2-H_2, Ar-N_2-O_2 microwave early afterglows [6].

The present paper is focused on Ar-N_2 early afterglow by directly introducing the discharge tube of 5 mm dia. inside the 5 litre reactor. By this way, it is expected to add the metastable $N_2(A)$ and $N_2(X, v > 13)$ molecules and N_2^+ ions to the N-atoms in the surface treatments as previously experimented [1] [2]. The studied active species are as in [6] the N and O-atoms, the $N_2(A)$ and $N_2(X, v > 13)$ metastable molecules and N_2^+ ions. The intensities emitted by the N_2 first positive (1^{st} pos.) and N_2 second positive (2^{nd} pos.) systems and by the NO_β bands are measured to obtain the mentioned active specie densities after NO titration to calibrate the N and O-atom densities [6]. The O-atoms are coming from air impurity in the discharge.

2. Experimental Setup and NO Titration

The experimental setup is changed in comparison to the one used in [6]. The dia. 5 mm discharge tube is now directly connected to the 5 litre reactor as shown in **Figure 1**. The Ar-N_2 microwave plasmas is always produced by a surfatron cavity at 2450 MHz, 100 Watt, 1 slm, but lowering the gas pressure from 8 Torr in [6] to 4 Torr to allow a satisfactory diffusion of the afterglow inside the 5 litre reactor.

The plasma is located inside the dia.5 mm tube with a length after the surfatron gap varying from about 5 cm in pure N_2 to 20 cm in the Ar-2%N_2 gas mixture. With a discharge tube length of 30 cm after the surfatron gap, the residence time before the afterglow in the 5 litre reactor is 3×10^{-3} s.

The optical emission spectroscopy across the reactor is performed by means of an optical fiber connected to an Acton Spectra Pro 2500i spectrometer (grating 600 gr/mm) equipped with a Pixis 256E CCD detector (front illuminated 1024 × 256 pixels).

The N-atom density is obtained from the I_{580} measured intensity after calibration by NO titration as described in [6].

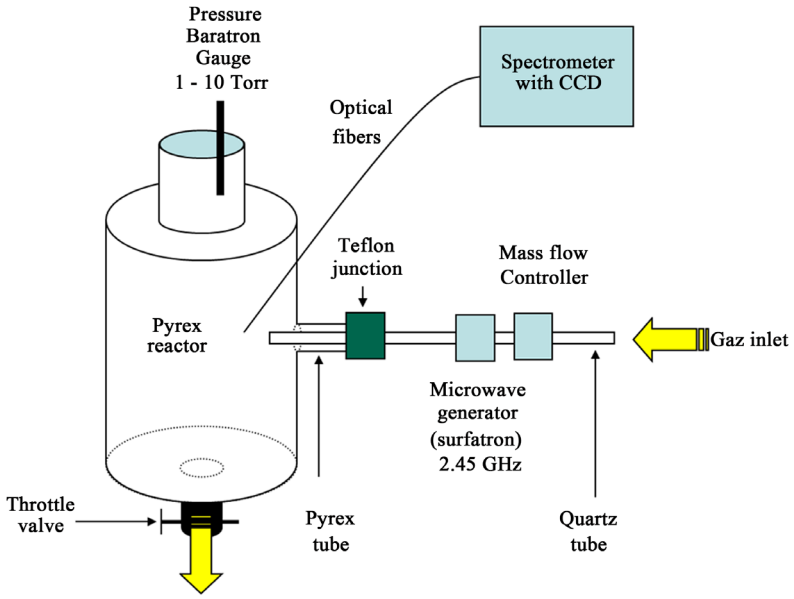

Figure 1. Microwave discharge and post-discharge reactor of 5 liters.

3. The Ar-N_2 Early Afterglow

3.1. N-Atom Density

As reported in [6], the pure late afterglow emission is produced by reaction R1 in **Table 1**.

The N_2 (580 nm) band head intensity (I_{580}^m) in arbitrary unit (a.u) was measured for constant parameters of the Acton spectrometer (grating 600 gr/mm, slit of 150 μm, integrating time 1 s).

I_{580}^m is then deduced from reaction R1 with v' = 11 and hυ = hc/λ (580 nm), as follows:

$$I_{580}^m = k_1 [N]^2 \quad (1)$$

with k_1 explicited in [4]-[6].

The reaction R1 produced with an excess of Ar atoms results in a change of the $N_2(B, v')$ distribution as compared to pure N_2 at a given a_{N+N} value. The N + N recombination coefficient a_{N+N} has been calculated in [6] in conditions of pink and late afterglows for Ar-xN_2 gas mixture with x from 2% to 100%.

Equation (1) becomes:

$$a_{N+N} I_{580}^m = k_1 [N]^2 \quad (2)$$

By NO titration,it has been verified the same k_1 value inside the error bars as for pure N_2 [6]:

$k_1 = 0.6\ (+/-\ 0.3)10^{-26}$ cm^6 counts/s with I_{580}^m in counts/s and [N] in cm^{-3}.

It is obtained $a_{N+N} = 0.9$ for pure N_2 and $a_{N+N} = 0.5$ for the Ar-2% N_2 mixture in the 5 litre reactor.

This result indicates that the early afterglow in N_2 is dominated by the N+N recombination as expressed by R1.

The N-atom density is then obtained in the 5 litre reactor by taking into account the change of diameter from 2.1 cm in the tube to 15 cm in the reactor.

It is reported in **Figure 2** the N-atom density variation with the %N_2 into Ar

A slow increase of N-atom density is found in the range 2% - 10% N_2 to reach a constant value of (5 - 6) × 10^{14} cm^{-3} between 10 and 100% N_2. The uncertainty on N-atom density is estimated to be 30% [6].

Table 1. Kinetic reactions in Ar-N_2 afterglow.

Reactions	
$N + N + (Ar\text{-}N_2) \rightarrow N_2(B, v') + (Ar\text{-}N_2)$ $N_2(B, v') \rightarrow N_2(A, v'') + h\upsilon_{580}$	R1
$N + O + (Ar\text{-}N_2) \rightarrow NO(B, 0) + (Ar\text{-}N_2)$ $NO(B, 0) \rightarrow NO(X, 8) + h\upsilon(320\ nm)$	R2
$N_2(A) + N_2(A) \rightarrow N_2(C, 1) + N_2(X)$ $N_2(C, 1) \rightarrow N_2(B, 0) + h\upsilon(316\ nm)$	R3
$N_2(A) + N_2(A) \rightarrow N_2(B, 11) + N_2$	R4
$N_2(A) + N_2(X, v > 13) \rightarrow N_2(B, 11) + N_2$	R5
$N_2(a') + N_2(a') \rightarrow e + N_2^+(X) + N_2(X)$	R6
$N_2^+(X) + N_2(X > 12) \rightarrow N_2^+(B) + N_2(X)$ $N_2^+(B, 0) \rightarrow N_2^+(X, 0) + hv(391\ nm)$	R7
$Ar^+ + N_2 \rightarrow Ar + N_2^+$	R8

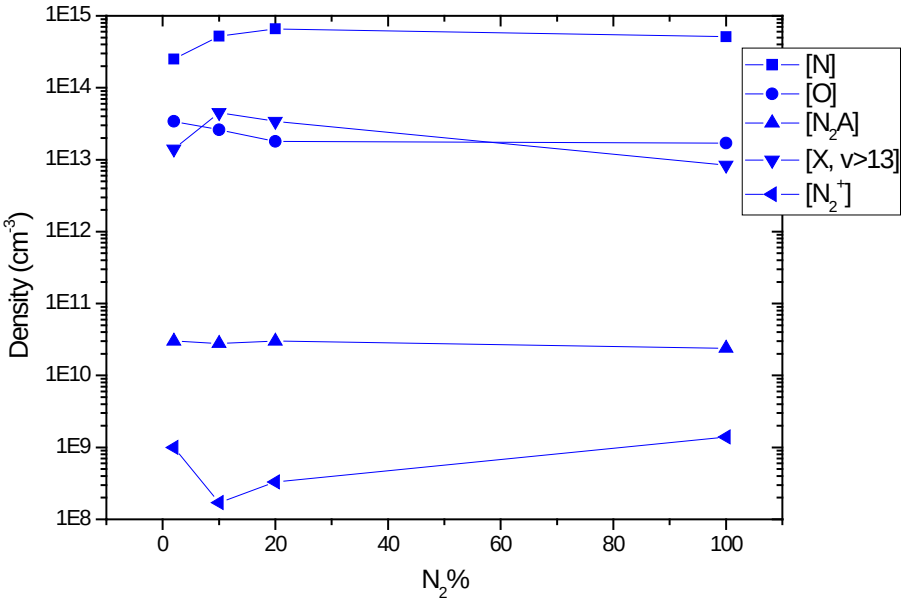

Figure 2. Active species density versus the $\%N_2$ into the Ar-N_2 early afterglow in the 5 litre reactor at 4 Torr, 1 Slm, afterglow time of 3×10^{-3} s, plasma 100 Watt.

3.2. Density of O-Atoms in Impurity in the Ar-N_2 Early Afterglow

The NO_β bands are presently observed as a result of the recombination of N and O atoms by reaction R2. In a similar way than for Equation (1), the NO (320 nm) measured band intensity (I_{320}^m) is deduced from reaction R2 as follows:

$$I_{320}^m = k_3[N][O] \tag{3}$$

The coefficients in k_3 are explicited in ref. 6 as for k_1.

The O atom density can be deduced from the N-atom density by considering the a_{N+N}. I_{580}^m / I_{320}^m ratio of reactions 2 and 3, as follows:

$$a_{N+N} \cdot I_{580}^m / I_{320}^m = k_4[N]/[O] \tag{4}$$

with $k_4 = k_1/k_3$.

After several NO titration experiments, it was found in [6]: $k_4 = 1(+/-0.4)$. From k_4 obtained by NO titration, the O-atom density in the Ar-N_2 early afterglow inside the reactor was determined by Equation (4) after measurements of $a_{N+N}\, I_{580}^m / I_{320}^m$ and [N] versus the N_2 percent into Ar. The results are reproduced in **Figure 2**. If the uncertainty on N-atom density is estimated to be 30% (see part 3.1), the experimental errors on O-atom density calculated from Equation (4), with the uncertainty on k_4 of 40% is 90% that is near the order of magnitude.

As shown in **Figure 2**, there is a slow decrease of the O-atom density from 3 to 2×10^{13} cm^{-3} between 2% to 100%N_2.

3.3. Density of $N_2(A)$ Metastable Molecules

It has been detected the $N_2(C, 1 \rightarrow B, 0)$ emission at 316 nm near the NO_β emission at 320 nm which is used as in [4]-[6] to determine the density of the $N_2(A)$ metastable molecule.

It is considered that the N_2 2^{nd} positive system in the early afterglow is produced by reaction R3.

The N_2 (316 nm) measured intensity (I_{316}^m) is then given by:

$$I_{316}^m = k_5\left[N_2(A)\right]^2 \tag{5}$$

with k_5 explicited in [6].

From Equations (3) and (5), it comes the following I_{320}^m / I_{316}^m intensity ratio:

$$I^{m}_{320}/I^{m}_{316} = k_6[N][O]/[N_2(A)]^2 \quad (6)$$

with $k_6 = k_3/k_5$. The $N_2(A)$ density is then obtained from equation (6) with the N and O atom densities previously determined.

As shown in **Figure 2**, the $N_2(A)$ density kept a constant value in the Ar-N_2 gas mixture. It is estimated that it is obtained the order of magnitude of $N_2(A)$ density in the range 10^{10} - 10^{11} cm^{-3}.

3.4. Density of $N_2(X, v > 13)$ Molecules

The production of $N_2(B, 11)$ by R1 in the early afterglow is less than 1 ($a_{N+N} < 1$).

Other collisional processes in the pink afterglow [7] also excite the $N_2(B)$ states, in addition to reaction R1.

For this other part $(1 - a_{N+N})$, it is considered the reactions R4 and R5 whose rate coefficients are reported in [4]-[6]. The contribution of reactions R4 and R5 on I^{m}_{580} is then written as follows:

$$(1-a_{N+N})I^{m}_{580} = k_{R4}[N_2(A)]^2 + k_{R5}[N_2(A)][N_2(X, v>13)] \quad (7)$$

where k_{R4}, k_{R5} are the rate coefficients of reactions R4, R5. As $a_{N+N}I^{m}_{580} = k_1[N]^2$, it is deduced:

$$(a_{N+N}/1-a_{N+N})\left(k_{R4}[N_2(A)]^2 + k_{R5}[N_2(A)][N_2(X, v>13)]\right) = [N]^2 k_1 \quad (8)$$

With the experimental values of a_{N+N} and of N and $N_2(A)$ densities, it is found that $(a_{N+N}/1-a_{N+N})k_{R4}[A]^2$ is about 2 orders of magnitude lower than $[N]^2k_1$.It results that Equation 8 can be simplified as:

$$(a_{N+N}/1-a_{N+N})k_{R5}[N_2(A)][X, v>13] = [N]^2 k_1 \quad (9)$$

From the obtained values of N-atom and $N_2(A)$ density, it was deduced the values of $[N_2(X, v > 13)]$ as reproduced in **Figure 2**.

It is observed about one order of magnitude lower $N_2(X, v > 13)$ density as compared to N values.

Such values of $[N_2(X, v > 13)]$ can be considered as an estimated value depending on the R5 rate coefficient.

3.5. Density of N_2^+ Ions

The emission of the N_2^+ band at 391 nm is observed in the present early afterglows. It is generally proposed [8] that the N_2^+, 391 nm band is produced in the pink afterglow by reactions R6 and R7.

The I^{m}_{391} intensity is then expressed as follows:

$$I^{m}_{391} = k_{10}[N_2^+][N_2, X, v>12] \quad (10)$$

with $k_{10} = c_{391} \cdot V \cdot A_{391} \cdot k_{R7} / \left(\upsilon^{R}_{N_2^+} + [N_2]k^{Q}_{N_2^+B,0}\right)$, where c_{391} is the spectral response of spectrometer, V is the detected afterglow volume, A_{391} the Einstein coefficient of the N_2^+ (391 nm) transition, k_{R7} the rate coefficient of reaction R7 with $k_{R7} = 4\times10^{-11}$ $cm^3 \cdot s^{-1}$ [9], $\upsilon^{R}_{N_2^+} = 1.7\times10^{7}$ s^{-1} and $k^{Q}_{N_2^+B,0} = 8.8\times10^{-10}$ $cm^3 \cdot s^{-1}$ [10].

By comparing the intensities of I^{m}_{316} from Equation (5) and I^{m}_{391} from equation (10), it is calculated:

$$I_{391}/I_{316} = k_{11}\left([N_2^+][N_2, X, v>12]/[N_2(A)]^2\right) \quad (11)$$

with k_{11} increasing from 6.6 10^{-2} in pure N_2 to 0.17 in Ar-2%N_2.

By assuming the equality $[N_2, X, v>12] = [N_2, X, v > 13]$, it is found a N_2^+ density which decreases from about 10^9 cm^{-3} in pure N_2 to 2×10^8 cm^{-3} in Ar-10%N_2 and increases again to 10^9 cm^{-3} in Ar-2%N_2. To verify that the N_2^+ ions are not coming from the end of a plasma jet at Ar-2%N_2, the measurements have also be performed 5 cm above in the 5 litre reactor, keeping about the same results.

Compared to published data [11] [12], the value of N_2^+ density in pure N_2 appears to be in the same order of magnitude.

4. Interest of Ar-N_2 Gas Mixture for Surface Treatments

It is reported in **Figure 3** the N/N_2, $N_2(X, v > 13)/N_2$, $N_2(A)/N_2$ and N_2^+ / N_2 density ratio versus the %N_2 into

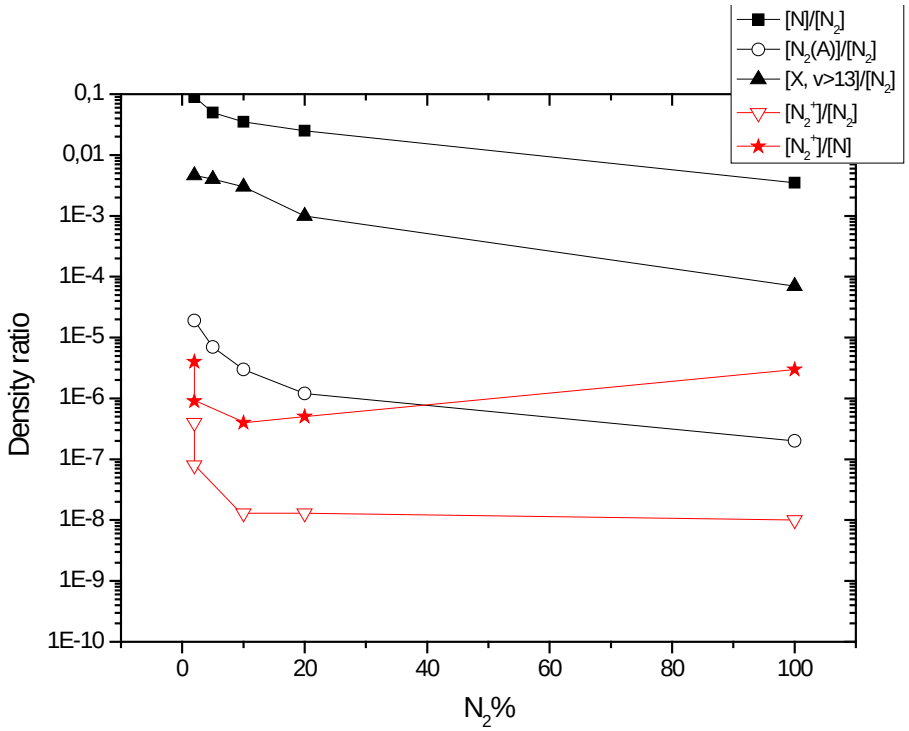

Figure 3. Density ratios of active species on N_2 versus the $\%N_2$ in the Ar-N_2 gas mixtures. In addition N_2^+ / N ratio.

Ar. Clearly, there is an interest of low $\%N_2$ to increase the active species density relative to N_2 if it can be considered that the Ar atoms have no influence on the surface processes.

The N_2^+ / N_2 density ratio is nearly constant from pure N_2 to Ar-10%N_2 with a new increase with Ar-2%N_2.

There is thus an interest of Ar-xN_2 gas mixtures with x = 2% - 20% for surface treatments with high N, N_2(A, Xv > 13) and N_2^+ density values (see **Figure 2**).

The N_2^+ / N density ratio decreased from pure N_2 to Ar-10%N_2 with an increase at Ar-2%N_2 to find again the value in pure N_2.

This increase of N_2^+ density for Ar-2%N_2 could be the result of the charge transfer R8 at the benefit of the N_2^+ ions [13].

5. Conclusions

Densities of N and O atoms (the O-are coming from air impurity), N_2(A) and N_2(X, v > 13) metastable molecules and N_2^+ ions have been determined in Ar-N_2 early afterglows of flowing microwave discharges at 1 slm, 4 Torr, afterglow time of 3×10^{-3} s and 100 W, after NO calibration.

The density of these active species are obtained by comparing the N_2 (580 nm), NO_β (320 nm), N_2 (316 nm) and N_2^+ (391 nm) band intensities and by writing the dominant kinetic equations.

It is found densities in the ranges of $(2 - 6) \times 10^{14}$ cm^{-3} for N-atoms, one order of magnitude lower for both N_2(X, v > 13) and O-atoms (coming from air impurity), of 10^{10} - 10^{11} cm^{-3} for N_2(A) and of 10^8 - 10^9 cm^{-3} for N_2^+.

The densities obtained by these line-ratio measurements are with an uncertainty of 30% for N-atoms and the order of magnitude for O-atoms and N_2(A) metastable molecules. Estimated densities values are obtained for the N_2(X, v > 13) metastable and N_2^+ ions which are depending on the kinetics reaction rates.

It is found that the main interest of N_2 dilution into Ar is to increase the N/N_2 dissociation from 0.5% in N_2 to about 10% in the Ar-2%N_2 which could be of interest for surface reactions of N-atoms with less N_2 molecules. The other $N_2(A)/ N_2$, $N_2(X, v > 13)/N_2$ density ratios are also increasing at low $\%N_2$ into Ar. It is not the case for the N_2^+ / N_2 and N_2^+ / N ratios which are constant or decreasing from pure N_2 up to 10%N_2.

References

[1] Villeger, S., Sarrette, J.P. and Ricard, A. (2005) Synergy between N and O Atom Action and Substrate Temperature in a Sterilization Process Using a Flowing N_2-O_2 Microwave Post-Discharge. *Plasma Process and Polymers*, **2**, 709-711. http://dx.doi.org/10.1002/ppap.200500040

[2] Villeger, S., Sarrette, J.P., Rouffet, B., Cousty, S. and Ricard, A. (2008) Treatment of Flat and Hollow Substrates by a Pure Nitrogen Flowing Post Discharge. Application to Bacterial Decontamination in Low Diameter Tubes. *European Physical Journal Applied Physics*, **42**, 25-32. http://dx.doi.org/10.1051/epjap:2007177

[3] Ricard, A., Gaboriau, F. and Canal, C. (2008) Optical Spectroscopy to Control a Plasma Reactor for Surface Treatments. *Surface and Coatings Technology*, **202**, 5220-5224. http://dx.doi.org/10.1016/j.surfcoat.2008.06.070

[4] Ricard, A., Oh, S.G. and Guerra,V. (2013) Line-Ratio Determination of Atomic Oxygen and N_2 Metastable Absolute Densities in an RF Nitrogen Late Afterglow. *Plasma Sources Science and Technology*, **22**, Article ID: 035009. http://dx.doi.org/10.1088/0963-0252/22/3/035009

[5] Ricard, A. and Oh, S.G. (2014) Densities of Active Species in N_2 and N_2-H_2 RF Pink Afterglow. *Plasma Sources Science and Technology*, **23**, Article ID: 045009. http://dx.doi.org/10.1088/0963-0252/23/4/045009

[6] Zerrouki, H., Ricard, A. and Sarrette, J.P. (2014) Determination of N and O-Atoms, of N_2(A) and N_2(X, v>13) Metastable Molecules and N_2^+ Ion Densities in the Afterglows of N_2-H_2, Ar-N_2-H_2 and Ar-N_2-O_2 Microwave Discharges. *Journal of Physics*: *Conference Series*, **550**, Article ID: 012045. http://dx.doi.org/10.1088/1742-6596/550/1/012045

[7] Levaton, J. and Amorim, J. (2012) Metastable Atomic Species in the N_2 Flowing Afterglow. *Chemical Physics*, **397**, 9-17. http://dx.doi.org/10.1016/j.chemphys.2011.11.010

[8] Sa, P.A., Guerra, V., Loureiro, J. and Sadeghi, N. (2004) Self-Consistent Kinetic Model of the Short Lived Afterglow in Flowing Nitrogen. *Journal of Physics D*: *Applied Physics*, **37**, 221-231. http://dx.doi.org/10.1088/0022-3727/37/2/010

[9] Piper, L.G. (1994) Further Observations on the Nitrogen Orange Afterglow. *Journal of Chemical Physics*, **101**, 10229-10236. http://dx.doi.org/10.1063/1.467903

[10] Kang, N., Lee, M., Ricard, A. and Oh, S.G. (2012) Effect of Controlled O_2 Impurities on N_2 Afterglows of RF Discharges. *Current Applied Physics*, **12**, 1448-1453. http://dx.doi.org/10.1016/j.cap.2012.04.009

[11] Sadeghi, N., Foissac, C. and Supiot, P. (2001) Kinetics of N_2(A) Molecules and Ionization Mechanisms in the Afterglow of a Flowing N_2 Microwave Discharge. *Journal of Physics D*: *Applied Physics*, **34**, 1779-1788. http://dx.doi.org/10.1088/0022-3727/34/12/304

[12] Ferreira, J.A., Stafford, L., Leonelli, R. and Ricard, A. (2014) Electrical Characterization of the Flowing Afterglow of N_2 and N_2/O_2 Microwave Plasmas at Reduced Pressure. *Journal of Applied Physics*, **115**, Article ID: 163303.

[13] Fehsenfeld, F.C., Ferguson, E.E. and Schmeltekopf, A.J. (1966) Thermal Energy Ion-Neutral Reactions Rates VI. Some Ar^+ Charge Transfer Reactions. *Journal of Chemical Physics*, **45**, 404-405. http://dx.doi.org/10.1063/1.1727351